A COMPARISON OF DIFFERENTIAL ROTATION MEASUREMENTS

(Invited Review)

JOHN G. BECK
W. W. Hansen Experimental Physics Laboratory, Stanford, CA 94305-4085, U.S.A.

(Received 30 July 1999; accepted 20 September 1999)

Abstract. Observers have long measured solar rotation with different techniques and obtained different results. This paper compares differential rotation measurements from four techniques: Doppler shift, Doppler feature tracking, magnetic feature tracking, and *p*-mode splittings. The different rotation rates measured by the first three techniques are interpreted as rotation rates of solar phenomena which depend on the properties and depth of that which is measured. This interpretation is supported by comparison with rotation measurements obtained from *p*-mode splittings except for Doppler features. The rotation rate of the plasma corresponds to the surface rate obtained by inversions; the rates of magnetic features correspond to the rotation rate at various depths within the convection zone. Supergranulation rotates at a rate greater than the maximum rotation rate within the convection zone, suggesting that supergranules are not simple convection cells anchored at a particular depth.

1. Introduction

Differential rotation is an obvious, yet poorly understood, solar phenomenon. As early as 1630, Christoph Scheiner noted that sunspots near the equator traverse the solar disk more rapidly than those near the poles. In 1863, Carrington used sunspots to produce the first measurement of differential solar rotation. Despite the long history of observations, solar differential rotation has yet to be adequately explained. What maintains it? How does it interact with the solar cycle? Does it vary, and if so by how much? If it does vary, what are the accelerating and braking mechanisms? There is still much work to be done before these questions can be answered. However, we are able to put many current observations into a coherent view of solar rotation (e.g., Rüdiger, 1989)

The first quantitative observations of solar rotation tracked sunspots across the solar disk: Carrington measured the latitude and longitude of thousands of sunspots from 1855 to 1861 at Redhill Observatory. He first observed that sunspots occur mainly in the band 6° to 35° north and south of the equator and that sunspots later in the solar cycle form closer to the equator than do earlier sunspots. Perhaps his most famous result was differential rotation which he found varied $\sim \sin^{7/4}\phi$, where ϕ is the heliographic latitude.

Later, with improved spectrographs, Doppler shifts were used to measure rotation. The early efforts involved taking the difference of Doppler measurements at the east and west limb. These were highly susceptible to noise from supergranulation and the limb redshift. The advent of photoelectric detectors improved

Solar Physics **191:** 47–70, 1999.

measurements by allowing for large numbers of disk images to be produced and analyzed, thereby reducing the effects of time-varying solar noise. The increased quality and quantity of data also made it easier to separate the limb red shift, which is symmetric about the central meridian, from the rotation which is anti-symmetric. However, spectroscopic measures must address the effects of scattered light, fringing and polarization.

Electronic detectors also improved feature-tracking methods of rotation measurement. Cross-correlations between high-resolution images taken at a high cadence can measure movements on short time scales, thereby reducing the effects of feature evolution. Digital images made additional magnetic features, such as the magnetic network, and Doppler features, such as supergranulation, available as tracers of solar rotation, too.

Helioseismology provided another method to determine solar rotation (Deubner, Ulrich, and Rhodes, 1979). Solar rotation causes frequency splitting between p modes of opposite azimuthal order. By measuring the splittings of many modes and using inverse methods, solar rotation as a function of depth and latitude can be inferred. Results from two helioseismology projects are included in this paper: the Global Oscillation Network Group (GONG) and the Michelson Doppler Imager (MDI). GONG data is acquired from six ground-based instruments located to provide nearly continuous observations of the Sun (Harvey *et al.*, 1996). The MDI instrument is on the SOHO spacecraft in a halo orbit about the L1 point, which provides nearly uninterrupted observations of solar oscillations (Scherrer *et al.*, 1995)

1.1. Differential rotation measurements and reference system

The determination of the solar rotation rate appears to be a trivial task, yet, after more than a century of observations discrepancies remain (e.g., Howard, 1984; Schröter, 1985). Rates vary depending upon the methods and type of data used; for example, magnetic features rotate faster than does the solar surface.

Heliographic longitude and latitude are a natural coordinate system for measuring differential rotation. Many measurements of differential rotation involve measurements of rotation at a variety of latitudes and a least-squares fit to some function of latitude. The determination of the rotation axis of the sun is required to calculate heliographic latitude and longitude – this is often found from values published by Carrington (1863). More accurate rotation measurements, however, require independent determination of the solar rotation axis.

Current measurements commonly express rotation in even powers of $\sin\phi$ such as

$$A + B\sin^2\phi + C\sin^4\phi. \tag{1}$$

In this formula, A is the equatorial rotation rate; B and C set the differential rate. One difficulty of producing a rotation law of the form in Equation (1) is that

coefficients B and C are coupled by an inverse correlation, first described by Duvall and Svalgaard (1978). The correlation between B and C leads to higher variance in the coefficients and renders comparisons between coefficients from different measurements more difficult.

One remedy to this problem is to fix the ratio C/B. Scherrer, Wilcox and Svalgaard (1980) set the ratio equal to 1.0; however, Ulrich *et al.* (1988) cited a ratio of 1.0216295 obtained by measuring the covariance of B and C. Many sunspot rotation measurements set $C = 0.0$, since the range of latitudes for which there are data is small. Whereas fixing the ratio C/B facilitates the comparison of coefficients obtained using the same ratio, it does not aid in comparison with differential rotation measurements using different fits. Further, this technique does not necessarily improve the variance in the coefficients.

Another approach, taken by Snodgrass (1984), is to orthonormalize the polynomial, using Gegenbauer polynomials. The cross-talk between the coefficients disappears almost completely. Since the Gegenbauer polynomials are linear combinations of $\sin^2\phi$, the coefficients can be easily translated to the form of Equation (1).

1.2. Differential rotation comparison

A search of solar rotation literature yields an overwhelming number of results. Comparing all rotation measurements is intractable and offers no advantage over comparing a representative subset. Most recent rotation measurements are consistent within 5%. However, when compared in greater detail, they reveal significant patterns among the variations. For example, spectroscopic measurements of plasma rotation are consistently lower than sunspot tracer measurements.

The measurements chosen for this comparison were selected owing to popular usage as well as illustrative examples. The spectroscopic measurements by Howard and Harvey (1970) and Snodgrass and Ulrich (1990) are frequently cited and used in analysis. Furthermore, these are part of a collection of solar rotation measurements from Mt. Wilson data, in which the improvement of techniques can be clearly seen. Newton and Nunn (1951) also made good measurements of sunspot rotation, which are often cited. Ward (1966) investigated the same data for variations due to young and recurrent sunspots. Nesme-Ribes, Ferreira, and Mein (1993) and others investigated solar cycle variations.

Explaining the differing results is facilitated by noting which component of the sun is measured by which technique. Bumba and Klvaňa (1994) noted that the interrelations of various phenomena of solar activity can be studied through comparison of the rotation rates. Rather than presenting a difficulty, the variation in results from different techniques is a tool for studying solar rotation.

Various theories of maintaining the differential rotation have been proposed: angular momentum transport by waves (e.g., Zahn, Talon, and Matias, 1997); angular momentum transport by Reynolds stresses (e.g., Gilman, 1977; Canuto, Minotti,

Schilling, 1994; Stix, 1989); angular momentum transport by meridional circulation (e.g., Schmidt, 1982). It is hoped that continued improvements in solar rotation measurements can unravel the mysteries of the mechanisms which produce and maintain it.

2. Spectroscopic Measurements

Solar rotation rates can be obtained from Doppler shifts of photospheric spectral lines. This yields the rotation of the plasma at the solar surface, as determined by the optical depth of the line. These measurements can be made throughout the solar cycle for nearly all latitudes (limited only by the projection angle at the poles), and so provide relatively complete measurements of solar rotation.

Doppler measurements have the disadvantage of being especially susceptible to scattered light due to the instrument and the atmosphere (Scherrer, Wilcox, and Svalgaard, 1980). Additionally, instrument polarization and spectrograph fringes contribute to the uncertainty of the measurement. For these reasons, instrument design and construction are crucial to high quality results.

Other factors affecting the measurement of the plasma rotation rate include large-scale velocity fields such as the limb red shift, torsional oscillations, and meridional flows (e.g., Howard, Boyden, and LaBonte, 1980; Ulrich *et al.*, 1988). In a properly aligned image, limb red shift and meridional flows are easily separated from the rotation, since they are symmetric about the central meridian and the rotation is anti-symmetric. However, a slight error in the orientation of the solar rotation axis can cause cross-talk between these flows. Torsional oscillations, perhaps more aptly named zonal flows, appear as variations in the rotation rate in latitudinal bands (Howard and LaBonte, 1980). The bands have an equatorward migration over the solar cycle, and can therefore be removed by observing over a suitably long period. Moreover, smaller-scale velocity fields, such as supergranules, contribute to the noise of the measurement.

2.1. METHODOLOGY

The most basic spectroscopic measurement of solar rotation is fit by least squares to the Doppler velocity at a constant latitude against the cosine of longitude, and in turn, fitting the rotation rates at each latitude to Equation (1). By combining these steps, additional terms may be added to fit for, and isolate, the limb redshift, meridional flows, and small-scale flows. The orientation of the rotation axis can be obtained from these fits.

Alternatively, independent measurements of large-scale velocities (including observer motion) may be subtracted from the image before fitting to the model.

TABLE I

Spectroscopic rotation measurements

Reference	A	B	C	Period	Notes
Hart (1954)	2.802			1950–1952	(1)
Howard and Harvey (1970)	2.78	−0.351	−0.442	1966–1968	(2)
	(0.025)	(0.016)	(0.027)		
Scherrer, Wilcox, and Svalgaard (1980)	2.901	−0.398	−0.398	1976–1979	(3)
Duvall (1982)	2.856			1978–1980	(4)
	(0.008)				
LaBonte and Howard (1982)	2.876	−0.312	−0.566	1967–1980	(5)
	(0.003)	(0.005)	(0.001)		
Howard *et al.* (1983)	2.867	−0.345	−0.477	1967–1982	(6)
	(0.001)	(0.002)	(0.002)		
Snodgrass (1984) A	2.838	−0.301	−0.526	1967–1984	(7)
	(0.002)	(0.003)	(0.004)		
Snodgrass (1984) B	2.836	−0.344	−0.504	1982–1984	(8)
	(0.001)	(0.003)	(0.006)		
Ulrich *et al.* (1988)	2.837	−0.410	−0.419	1967–1987	(9)
	(0.007)	(0.004)	(0.004)		
Snodgrass and Ulrich (1990)	2.851	−0.343	−0.474	1967–1984	(10)
	(0.006)	(0.005)	(0.007)		

All coefficients are in μrad s^{-1}, quantities in parentheses are errors.

(1) Oxford data – equatorial rotation rate only.

(2) MWO data.

(3) WSO data (with correction of 0.55% per Snodgrass, Howard, and Webster (1984)).

(4) KPNO data – equatorial rotation rate only.

(5) MWO data.

(6) MWO data – with scattered light correction.

(7) MWO data – 'all data' orthonormalized with Gegenbauer polynomials.

(8) MWO data – 'best data' orthonormalized with Gegenbauer polynomials.

(9) MWO data, extension of Howard *et al.*, 1983.

(10) MWO data – scattered light correction.

KPNO = Kitt Peak National Observatory, McMath Telescope.

MWO = Mt. Wilson Observatory, 150-foot tower.

WSO = Wilcox Solar Observatory.

2.2. Comparison of measurements

There have been many efforts over the decades to measure the rotation rate of the photospheric plasma. The measurements compared here are listed in Table I.

Some of the rotation measurements cited in this comparison were chosen due to the widespread application (e.g., Howard and Harvey, 1970; Snodgrass and Ulrich, 1990). Some results are extensions of previous studies, such as LaBonte and Howard (1982), Howard *et al.* (1983), Snodgrass (1984), and Ulrich *et al.* (1988).

It should be noted that most of these results were obtained from Mt. Wilson data. These data were scanned in boustrophedonic manner over a period of 20 to 90 min at the 150-foot tower. Details of operations can be found in Howard, Tanenbaum, and Wilcox (1968) and in Ulrich *et al.* (1988).

The tables of coefficients are in μrad s^{-1}. However, the plots also include scales of nHz, degrees per day, and period in days – all measurements are of the sidereal rotation rate. Some of the measurements only determined the equatorial rotation rate, and in these cases only the A coefficient is indicated. The error bars on these measurements are either provided by the authors or calculated from the standard deviation of the values published.

2.3. Discussion of measurements

Plots of the rotation measurements from Table I are shown in Figures 1 and 2. The equatorial measurements are indicated as single points plotted near the vertical axis. It should be noted that the error bars become larger at high latitudes owing to reduced signal strength, so the rotation rate of the poles is not well determined. Accurate measurement of polar rotation remains an active quest (e.g., Birch and Kosovichev, 1998; Riehokainen, Urpo, and Valtaoja, 1998; Scherrer *et al.*, 1997). Note that all of the measurements after 1980 are within 0.04 μrad s^{-1} (about 1.5%). This amounts to a variation (at the equator) of 28 m s^{-1}. Therefore the confidence in these measurements is high, but there is still some disagreement between them.

The Doppler-shift measurements are susceptible to many problems which typically reduce the differential rotation, such as scattered light. Ulrich *et al.* (1988) discusses some of these. The treatment of these phenomena is critical to producing an accurate measurement, and is discussed in detail in Ulrich *et al.* (1988), Snodgrass (1984) and Snodgrass and Ulrich (1990).

3. Tracer Measurements

The earliest studies of solar rotation observed the movement of sunspots across the visible disk; the sunspots were used as tracers and were assumed to co-rotate with the Sun. Other solar features which are useful as tracers include plages, faculae, coronal holes, supergranules and the recently observed giant cells (Beck, Duvall, and Scherrer, 1998; Ulrich, 1998). The measured rotation rate depends on the type

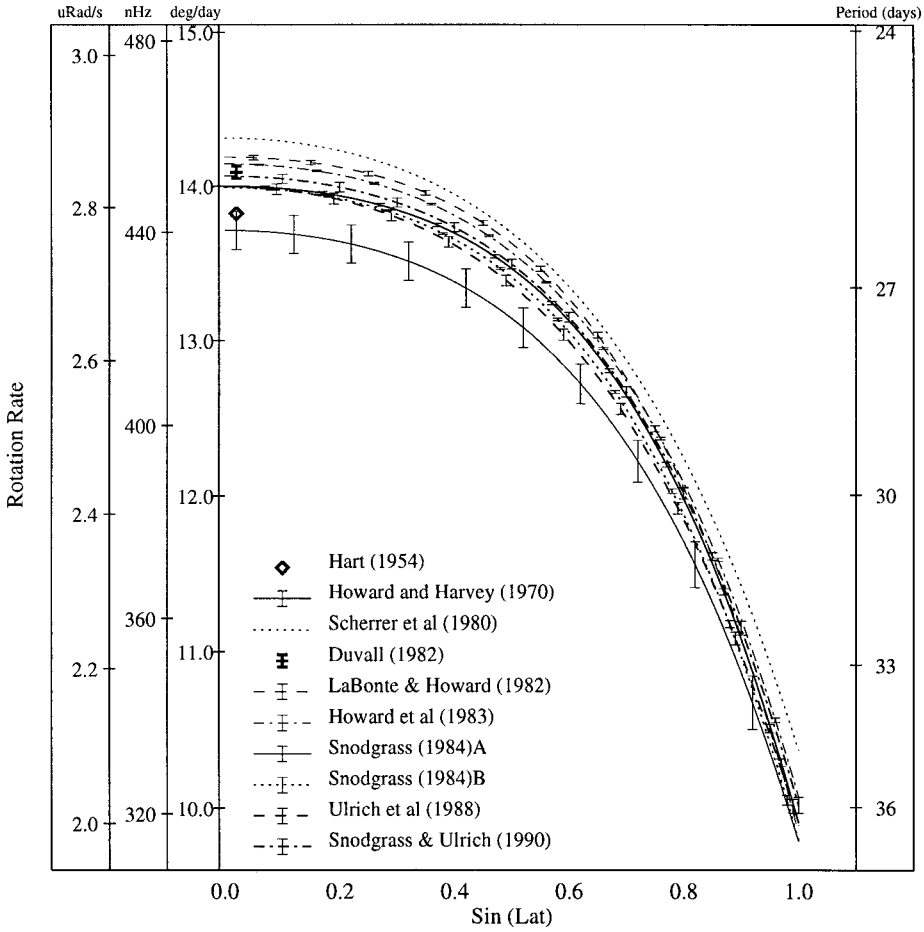

Figure 1. Spectroscopic rotation. Plots of differential rotation curves from coefficients listed in Table I. The low value of Howard and Harvey (1970) has been attributed to scattered light. The Snodgrass B measurement is flatter at mid-latitudes than Snodgrass A, which used some of the data used by Howard and Harvey. Snodgrass and Ulrich (1990) lies close to Snodgrass A except at the equator. With the exception of the first three curves listed in the table, all of these curves lie within 1.5%. It is probably not significant that the variation in these plots decreases at higher latitudes because that is where the uncertainty of the measures is largest.

of feature used and, typically, does not match the rotation of the photospheric plasma. The solar rotation rates obtained from tracers are listed in Table II. Notably, all of the features used for rotation tracers, except giant cells, are seen to be associated with magnetic fields. Deubner, Ulrich, and Rhodes (1979) observed that the rotation rate below the solar surface matched that of sunspots. Features associated with magnetic fields penetrating into the convection zone may rotate at a rate corresponding to some characteristic depth, which may be termed the anchor depth of that feature (Nesme-Ribes, Ferreira, and Mein, 1993).

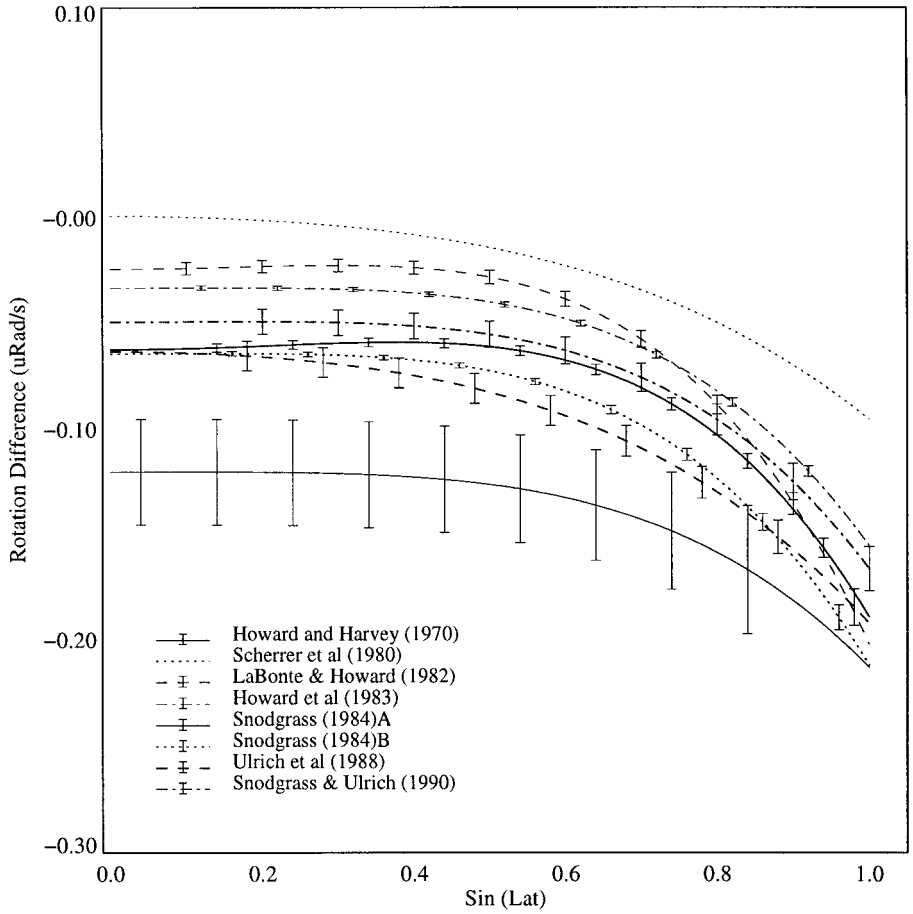

Figure 2. Spectroscopic rotation differences. A 'standard' differential rotation curve $(2.90 - 0.35(\sin^2\phi + \sin^4\phi))$ has been subtracted from curves plotted in Figure 1 to better show the differences. The variation of curvature reflects the variation of the measure of differential rotation. The plots of Howard *et al.* (1983), Snodgrass (1984) and Snodgrass and Ulrich (1990) show the most similar differential rotation curve; although the absolute rates of rotation are quite different between these three. Note that few of these measurements are consistent within error bars.

3.1. METHODOLOGY

Tracer measurements of solar rotation require dividing a difference in angular position by a difference in time. There are different approaches to obtaining these differences: measuring the time when the tracer crosses a specific position, measuring the position of the tracer at known times, cross-correlating images separated by a known time.

The first approach typically measures the rotation period of the tracer: the time from one central meridian crossing to the next. This was the method employed

by Newton and Nunn (1951). An important disadvantage of this technique is that short-lived features cannot be used as tracers, causing a selection effect.

The second approach was used by Carrington in 1863; he measured heliographic latitude and longitude for many sunspots from daily sunspot drawings and calculated the differential rotation from those measurements. This method requires an accurate knowledge of image scale and sufficient spatial resolution to determine position precisely; additionally, the temporal sampling must be at intervals shorter than the evolution time scale in order to obtain consistent measurements.

The cross-correlation method has higher demands on spatial and temporal sampling and is difficult to apply to historical sunspot drawings. However, it is more objective when measuring the displacement of features distributed over a relatively large area. Furthermore, the correlation coefficient provides a measure of the confidence of the measurement.

All of these methods are sensitive to the evolution of the features. The image cadence must be high enough that features are similar between successive images.

3.2. SUNSPOT ROTATION MEASUREMENTS

Sunspots are the most widely used tracer of solar rotation. These features are visible in white-light images, magnetograms and filtergrams of a variety of spectral lines. In fact, the oldest solar data still used are sunspot drawings.

A three-term fit to Carrington's sunspot measurements of longitude and latitude is supplied for comparison. This measurement should not be confused with the Carrington rotation rate of 2.865 μrad s^{-1} (or a period of 25.38d sidereal).

Newton and Nunn (1951) used data from the *Greenwich Heliographic Results* to measure the rotation rate of recurrent sunspots. Using photographic images, they determined the time a sunspot crossed the central meridian on two successive rotations, thus measuring the solar rotation period.

Ward (1966) investigated the selection effect of recurrent sunspots using Greenwich data. The rotation rate of recurrent sunspots was measured and compared with the rotation rate of all sunspots. Ward also found that dividing sunspots by area or morphology produced different rotation rates. Tang (1981) investigated the bias of using low-latitude sunspots. Zappala and Zuccarello (1991) measured the rotation rates of sunspots of various ages, finding recurrent sunspots rotate 0.06 μrad s^{-1} more slowly than 2-day-old sunspots. Howard, Gilman, and Gilman (1984) used the Mt. Wilson sunspot photographs from 1921–1982 and divided sunspots into small, medium and large spots (using cutoffs of 5 and 10 millionths of a solar hemisphere). Snodgrass and Ulrich (1990) used all magnetic features visible in Mt. Wilson magnetograms as solar rotation tracers.

3.3. MAGNETIC FIELD ROTATION MEASUREMENTS

Komm, Howard and Harvey (1993b) and Snodgrass and Ulrich (1990) measured the magnetic rotation rate by cross-correlating magnetograms from successive days.

TABLE II

Tracer rotation measurements

Reference	A	B	C	Period	Notes
Carrington (1863)	2.9	−0.732	0.505	1855–1861	(1)
	(0.01)	(0.02)	(0.03)		
Newton and Nunn (1951)	2.905	−0.598		1934–1944	(2)
Ward (1966) (recurrent)	2.9044	−0.543		1878–1944	(3)
	(0.0006)	(0.016)			
Ward (1966) (all spots)	2.9337	−0.543		1905–1954	(4)
	(0.0012)	(0.012)			
Tang (1981)	2.903	−0.525		1978–1979	(5)
Howard, Gilman, and Gilman (1984) A	2.939	−0.5796		1921–1982	(6)
	(0.001)	(0.01)			
Howard, Gilman, and Gilman (1984) B	2.917	−0.5284		1921–1982	(7)
	(0.002)	(0.018)			
Howard, Gilman, and Gilman (1984) C	2.885	−0.5325		1921–1982	(8)
	(0.0036)	(0.034)			
Zappala and Zuccarello (1991) A	2.9715	−0.436		1874–1976	(9)
	(0.002)	(0.02)			
Zappala and Zuccarello (1991) B	2.903	−0.615		1874–1976	(10)
	(0.002)	(0.026)			
Komm, Howard, and Harvey (1993b)	2.913	−0.405	−0.422	1975–1991	(11)
	(0.004)	(0.027)	(0.030)		
Snodgrass and Ulrich (1990)	2.879	−0.339	−0.485	1984–1987	(12)
	(0.002)	(0.013)	(0.021)		
Duvall (1980)	2.974			1979	(13)
	(0.014)				
Snodgrass and Ulrich (1990)	2.972	−0.484	−0.361	1966–1987	(14)
	(0.01)	(0.04)	(0.05)		

All coefficients are in μrad s^{-1}, quantities in parentheses are errors.

(1) From three-term fit to Carrington's original measurements.

(2) Using sunspots with lifetime $>$ 1 solar rotation.

(3) Using recurrent sunspots (lifetime $>$ 1 solar rotation).

(4) Using all sunspots.

(5) Using sunspots at high latitudes.

(6) Using whitelight images of sunspots with area $<$ 5 (in mHem).

(7) Using whitelight images of sunspots with 5 $<$ area $<$ 10 (in mHem).

(8) Using whitelight images of sunspots with 10 $<$ area (in mHem).

(9) Using only young sunspots.

(10) Using only recurring sunspots.

(11) Using correlation of KPNO magnetograms.

(12) Using correlation of daily MWO magnetograms.

(13) Equatorial rotation rate of supergranules from KPNO dopplergrams.

(14) Differential rotation of supergranules from MWO daily dopplergrams.

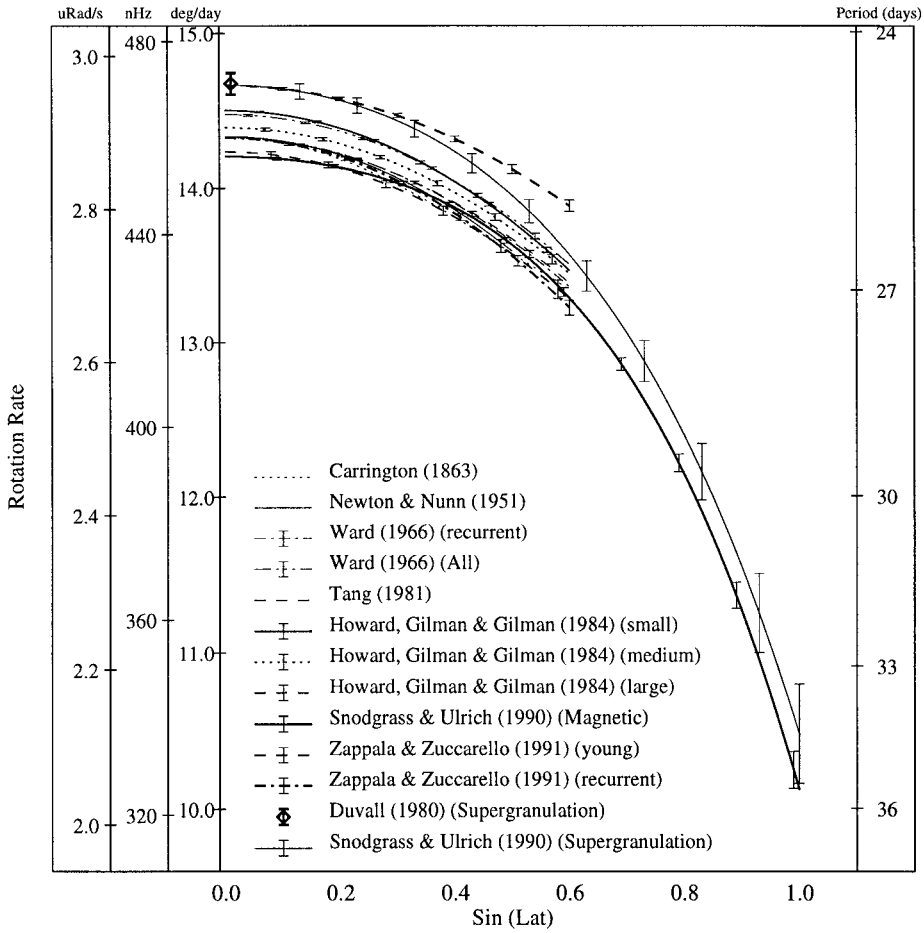

Figure 3. Tracer rotation measurements of differential rotation of tracers from coefficients listed in Table II. Not all curves extend to the highest latitude since few sunspots occur above 40° latitude. The two curves extending to high latitudes are the magnetic field and supergranulation rotation curves from Snodgrass and Ulrich (1990). The highest rotation rates are for supergranulation and young sunspots. Recurrent and larger sunspots have lower rotation rates.

The former study used Kitt Peak magnetograms with 2″ resolution; the latter used Mt. Wilson magnetograms binned to 34×34 pixels. The smaller scale measurement results in a greater rotation rate.

Meunier (1999) used MDI magnetograms with a resolution of 2″, separated by 96 minutes. The reported equatorial rates were 2.897 ± 0.004 μrad s^{-1} during the low activity period and 2.890 ± 0.004 μrad s^{-1} at high activity. These results lie midway between the results of the previous two studies.

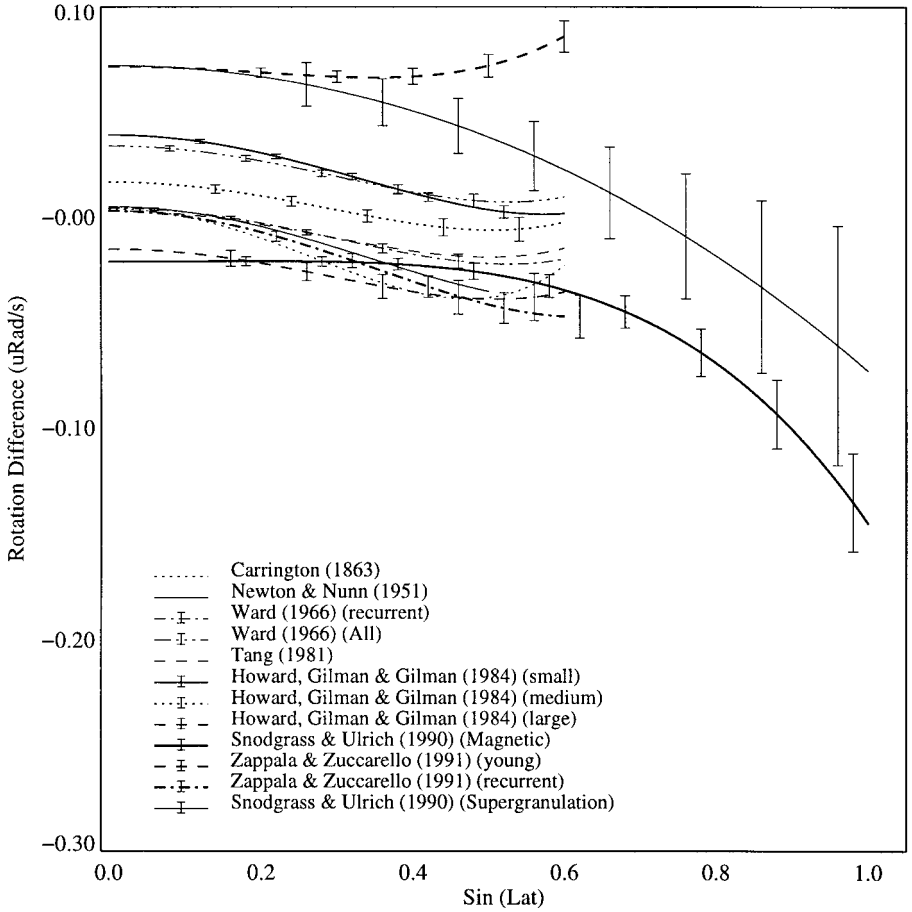

Figure 4. Tracer rotation differences. A 'standard' differential rotation curve $(2.90 - 0.35(\sin^2\phi + \sin^4\phi))$ has been subtracted from plots shown in Figure 3 to better show the differences. The variation of curvature reflects the variation of the measure of differential rotation. Young sunspot and supergranulation rotation are the higher plots. The shape of the differential rotation curves for sunspots are different than the shapes of the curves from Snodgrass and Ulrich (1990) which used supergranules or all magnetic features as tracers and extended to high latitudes.

3.4. SUPERGRANULATION ROTATION MEASUREMENTS

It is appropriate that supergranules were first observed by Hart (1954) while trying to measure the equatorial rotation rate of the sun and that Duvall (1980) later used supergranules to determine the equatorial rotation rate of the sun. Only two supergranule rotation measurements, Duvall (1980) and Snodgrass and Ulrich (1990), have been included in this comparison.

Duvall measured supergranule rotation by cross-correlating equatorial scans, with a resolution of $2''$ near the east and west limbs of the Sun. The scans were

temporally averaged to reduce the effects of p modes and granulation. The reported results were the average of results comparing scans separated by less than 10 hours and results of scans separated by more than 20 hours. Whereas the longer separations allowed for greater precision in change in position, the correlation coefficients were approximately half as large as the shorter separations. It is not surprising that both measurements have the same uncertainty.

Snodgrass and Ulrich (1990) measured rotation by cross-correlating daily, coarse-array images projected in heliographic longitude and latitude (34×34 pixels), which were detrended for rotation and limb red shift. The predominant signal was found to be from supergranulation, although supergranules were not resolved in these images. They reported rotation rates over the range of $\pm 70^\circ$ latitude.

3.5. Comparison of measurements

The four main conclusions which can be drawn from Figures 3 and 4 are: supergranules rotate faster than most sunspots, young sunspots rotate faster than recurrent sunspots, small sunspots rotate faster than large sunspots, and the shape of the differential rotation curve of sunspots differs from that of supergranules and that of all magnetic features.

The high rate of rotation for supergranules is quite striking, and will be discussed in detail in subsequent sections. The variation of sunspot rotation rates is an issue of increasing interest. Ward (1966) and Zappala and Zuccarello (1991) determined that young sunspots rotate 2.4% faster than recurring spots; Howard, Gilman and Gilman (1984) found that small sunspots rotate 1.8% faster than large sunspots. Beyond the results plotted, Balthasar, Schüssler, and Wöhl (1982) have measured a braking effect of 0.8 to 0.3 m s^{-1} per day, and concluded that spots are decelerated by the aerodynamic drag of the plasma. Gilman and Howard (1985) found that leader spots rotate 0.7% faster than follower spots. Also, it has been observed by Wilcox *et al.* (1970), Snodgrass (1983), Antonucci, Hoeksema, and Scherrer (1990) and Erofeev (1996) that there are two magnetic rotation rates: a rigid rotation and a differential rotation. Wilcox *et al.* (1970), reported a rigid rotation rate of 2.889 μrad s^{-1}, which is comparable to the equatorial rotation rates cited in Table II.

Rhodes *et al.* (1990) suggested that the rotation rate of a sunspot corresponds to the rotation of the plasma at the anchor depth of the spot. This may explain the observed variations in sunspot rotation rates: perhaps the anchor depth depends on the age and size of the sunspot. Nevertheless, before developing models to explain these observations, it is important to ask if these variations are truly significant.

For example, how do these variations compare with variations over the solar cycle? There have been many investigations into rotation rate variations due to the solar cycle. Gilman and Howard (1984) found a 3% peak in rotation rate at both solar minimum and maximum. Nesme-Ribes, Ferreira and Mein (1993) as well as Komm, Howard and Harvey (1993a) obtain consistent results of variations of 1%

in rotation over the solar cycle, finding that early cycle spots rotate more slowly than late cycle spots. However, sunspots tend to occur at higher latitudes early in the solar cycle and at lower latitudes later in the solar cycle so the comparison is done at latitudes with little or no activity. Ulrich and Bertello (1996) measured the magnetic rotation rate and found no solar cycle dependent fluctuations in the magnetic rotation rate. Meunier (1999) studied motions of magnetic features at all latitudes and reported finding a 0.5% variation in rotation from a period of low activity to high activity. Additionally, Kambry and Nishikawa (1990), found a variation of 2.5% between solar cycles 19 and 20.

The variations between young and recurring spots as well as the variations between small and large spots are approximately as large as the variations within a solar cycle. These variations appear to be significant.

4. Helioseismology Measurements

Helioseismology has made it possible to make inferences about the rotation of the solar interior. The Sun oscillates simultaneously in millions of modes of acoustic oscillation, termed p modes, which carry information about the sun's interior to the surface (Ulrich, 1970). Inversions of frequency measurements of p modes have produced maps of rotation beneath the surface of the Sun, which show that differential rotation extends deeply into convective zone, varying less with depth than with latitude. However, there is a small subsurface shear layer in which rotation increases with depth, peaking at 0.93 $R_\odot$. These results have provided a much better glimpse of differential rotation in the convection zone, and help us sort out the variety of surface rotation measurements.

4.1. METHODOLOGY

Helioseismology uses measurements of p-mode frequencies to infer properties of the solar interior. Each mode can be identified by spherical harmonic indices: n, l, m, where n is the radial order and l and m are the degree and azimuthal order of spherical harmonic $Y_l^m(\theta, \phi)$, describing the angular dependence of the mode. Note that m ranges from $-l$ to l. Each mode has a sinusoidal time dependence with cyclic frequency ν_{nlm}. In a non-rotating star, the frequency ν_{nlm} would be independent of m, so the multiplets of $2l + 1$ modes would have identical frequencies. Rotation induces a splitting, $\Delta\nu_{nlm} = (\nu_{nl(+m)} - \nu_{nl(-m)})$, which is the difference between modes of the same multiplet. The splittings are related to the underlying rotation profile by the equation

$$\Delta\nu_{nlm} = \iint K_{nlm}(r, \phi)\, \Omega(r, \phi)\, r\, \mathrm{d}r\, \mathrm{d}\phi\,, \tag{2}$$

where r is the distance from the center, ϕ is latitude, $\Omega(r, \phi)$ is the rotation at r and ϕ, and the functions $K_{nlm}(r, \phi)$ are mode kernels, are essentially known quantities once a solar model is specified.

The term 'inversion' refers to inferring the property of the Sun, $\Omega(r, \phi)$, from frequency measurements, $\Delta\nu_{nlm}$. This can be done in a number of ways, including a regularized least-squares fit (RLS), or optimally localized averages (OLA). Further discussion of inversion techniques can be found in Schou, Christensen-Dalsgaard, and Thompson (1994) and in Schou *et al.* (1998).

4.2. ROTATION MEASUREMENTS

The results of inversion of GONG frequency splittings were published by Thompson *et al.* (1996) and the results of MDI frequency splitting inversion have been published by Schou *et al.* (1998). These results are shown in Figure 5. The differential rotation can be seen throughout most of the convection zone.

Although there are some differences in details between the GONG and the MDI rotation inversions, they are in agreement for most of the convection zone. Figures 6 and 7 show slices at various depths within the convection zone for the MDI and GONG results. The GONG and MDI results are within error bars for latitudes below 55°.

Notably, the maximum rotation rate is at a depth of 0.93 $R_\odot$ for lower latitudes. Above 55°, the depth of the peak rotation grows deeper. At 65°, the peak depth nears 0.80 $R_\odot$.

The GONG and MDI rotation inversions display remarkable agreement. Therefore it is reasonable to compare surface rotation measurements to either inversion result.

5. Comparison of Helioseismology and Surface Rotation Measurements

The helioseismology rotation results are compared to a subset of the spectroscopic and tracer measurements discussed in previous sections. The Snodgrass and Ulrich (1990) supergranule magnetic spectroscopic measurements are used because these are three different measurements from the same set of observations. The Duvall supergranule rotation measurement is used, as are the sunspot measurements of Newton and Nunn (1951), Ward (1966), Zappala and Zuccarello (1991) and Howard, Gilman, and Gilman (1984).

These measurements provide us with a comparison of the plasma and supergranulation rotation rates with rotation in the convection zone. Further, the measurements of sunspot rotation for different sunspot ages, as well as different sunspot sizes, afford us a means to compare depths with sunspot properties.

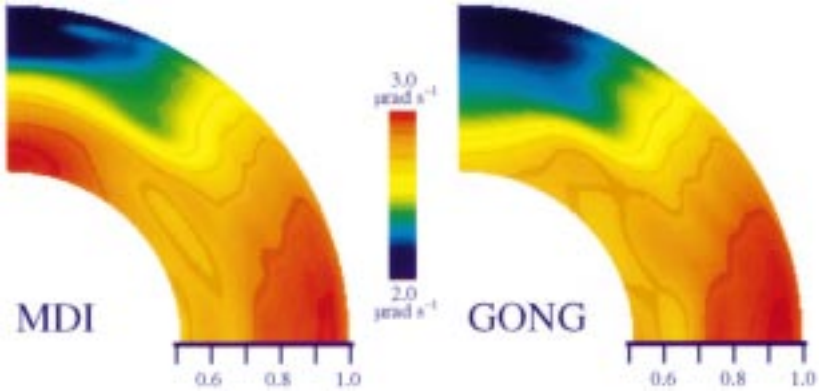

Figure 5. MDI and GONG inversions of solar rotation. These maps show the differential rotation as a function of latitude and depth inferred from inversion of MDI (Schou *et al.*, 1998) and GONG (Thompson *et al.*, 1996) p-mode frequency measurements. These maps are oriented so that the rotation axis is vertical, with the pole at the top and the equator horizontally along the bottom. The tick marks along the horizontal edges are at 0.1 $R_\odot$ intervals. The contours are at intervals of 0.10 μrad s^{-1}. The depth of most rapid rotation is at 0.93 $R_\odot$ at the equator. At mid-latitudes, the contours run radially outward through most of the convection zone. The GONG results are from data obtained between October 1995 to February 1996; the MDI results are from data from May 1996 through October 1996.

5.1. SUNSPOT ROTATION AND ANCHOR DEPTH

There is a clear trend of sunspot rotation: smaller spots rotate faster than larger spots; younger spots rotate faster than older spots. In Figure 8, the spot rotation rates are plotted along with the results of inversion for four selected latitudes.

At all four latitudes shown, the rates for young sunspots measured by Zappala and Zuccarello (1991) exceed the peak rotation rate obtained by inversions. At first this seems completely inconsistent, especially since the GONG and MDI inversions give the same answer. However, an artifact of inversions is that sharp features (such as the tachocline at the base of the convection zone) are smoothed. Because the kernel has a finite extent in latitude and in depth, it tends to reduce and broaden peaks. It is possible that the peak in the rotation rate is higher and narrower than that shown by the GONG and MDI inversions so the rotation young sunspots may not, in fact, exceed the maximum rotation rate within the convection zone.

Interestingly, the young spot rate corresponds to a depth of 0.93 $R_\odot$ whereas the recurrent spots measured by Zappala and Zuccarello correspond to a depth of 0.80 $R_\odot$ or 0.98 $R_\odot$. Recurrent spots correspond to either a level deep within the convection zone or just below the surface. Most magneto-hydrodynamic theories suggest that magnetic fields associated with sunspots tend to rise due to buoyancy, so it seems more consistent to pick the shallower depth.

The consideration of sunspot size yields a similar conclusion; the smaller spots rotate at a rate which corresponds to a depth near the rotation peak; however larger

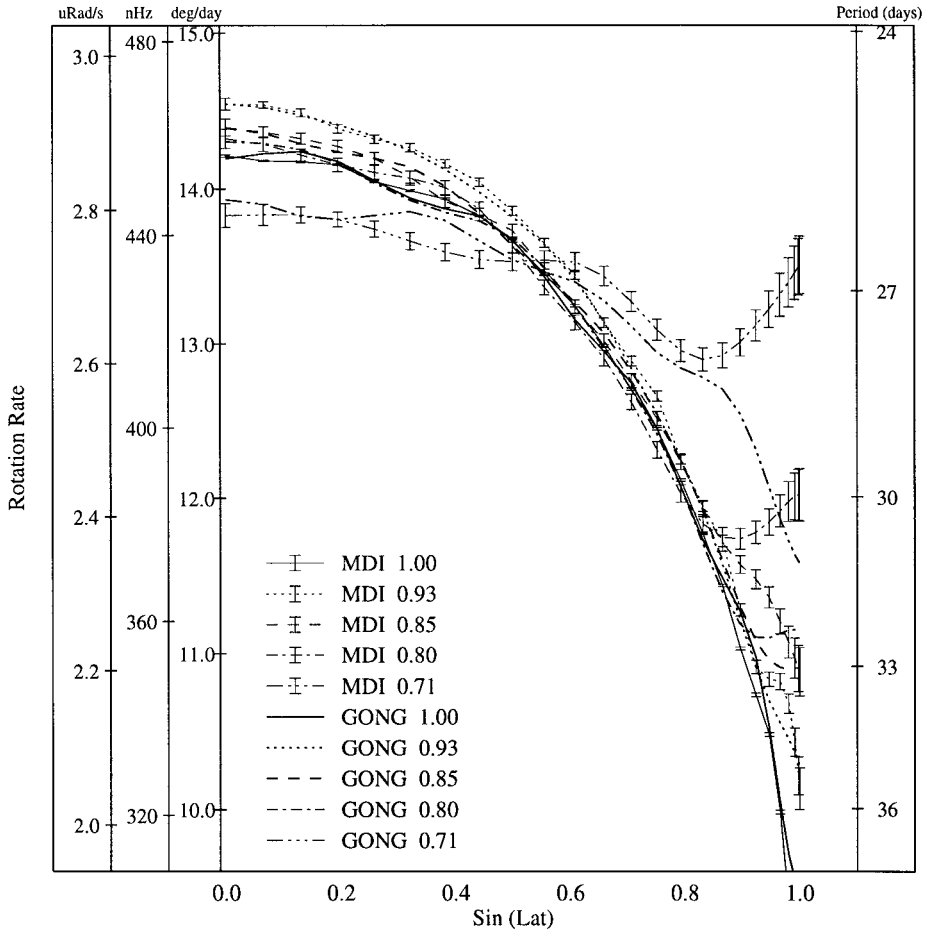

Figure 6. MDI and GONG differential rotation curves at various depths. By extracting curves at constant depths from the inversion of MDI (Schou *et al.*, 1998) and GONG (Thompson *et al.*, 1996) *p*-mode frequency measurements, the latitudinal dependence of rotation can be seen at several depths. Each curve is labeled according to the source of measurement and the depth (in solar radius, $R_\odot$). Note that the rotation increases from the surface down until it reaches a peak at 0.93 $R_\odot$. The depth 0.71 $R_\odot$, which corresponds to the base of the convection zone, rotates much more slowly than the surface.

spots are either deeper (perhaps as deep as 0.71 $R_\odot$, at the base of the convection zone) or just beneath the surface.

However, D'Silva and Howard (1994) reported that the rotation rates of sunspots could be explained by interaction of Coriolis force, drag, magnetic buoyancy and magnetic tension. Although flux tube dynamics may affect sunspot rotation rates, the effect of anchor depth on sunspot rotation cannot be ignored.

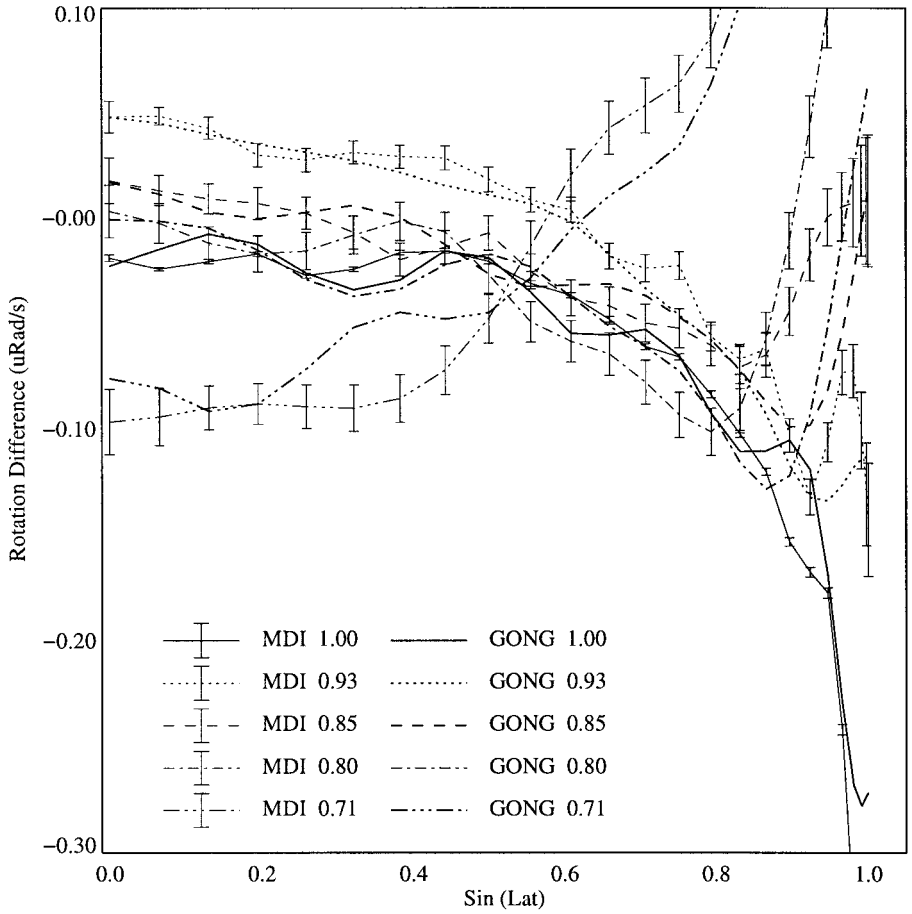

Figure 7. MDI and GONG differential rotation curve differences. Subtracting the 'standard' rotation $(2.90 - 0.35(\sin^2\phi + \sin^4\phi))$ from the curves plotted in Figure 6 shows the trends much more clearly. The results from the inversion of MDI (Schou *et al.*, 1998) and GONG (Thompson *et al.*, 1996) inversions typically match within error bars, showing that these results are repeatable.

5.2. SUPERGRANULE ROTATION AND ANCHOR DEPTH

Figures 9 and 10 show that the supergranulation rotation rate exceeds the maximum rotation rate within the convection zone (corresponding to a depth of 0.93 $R_\odot$). The error bars of Figure 10 show that the difference is $\geq 2\sigma$ at low latitudes.

Typical theoretical models of supergranules (e.g., Simon and Weiss, 1968) estimated a depth of approximately one-half of the horizontal extent which would be 15 000 km. Further, Duvall (1998) applied the technique of time-distance helioseismology to the study of supergranules and found evidence that the cells have a depth of only 8000 km. Using the deeper estimate, supergranules would be anchored at 0.98 $R_\odot$ which rotates far too slowly to match the supergranulation rate. The strong shear in the rotation rate from the surface down to 0.93 $R_\odot$ at low

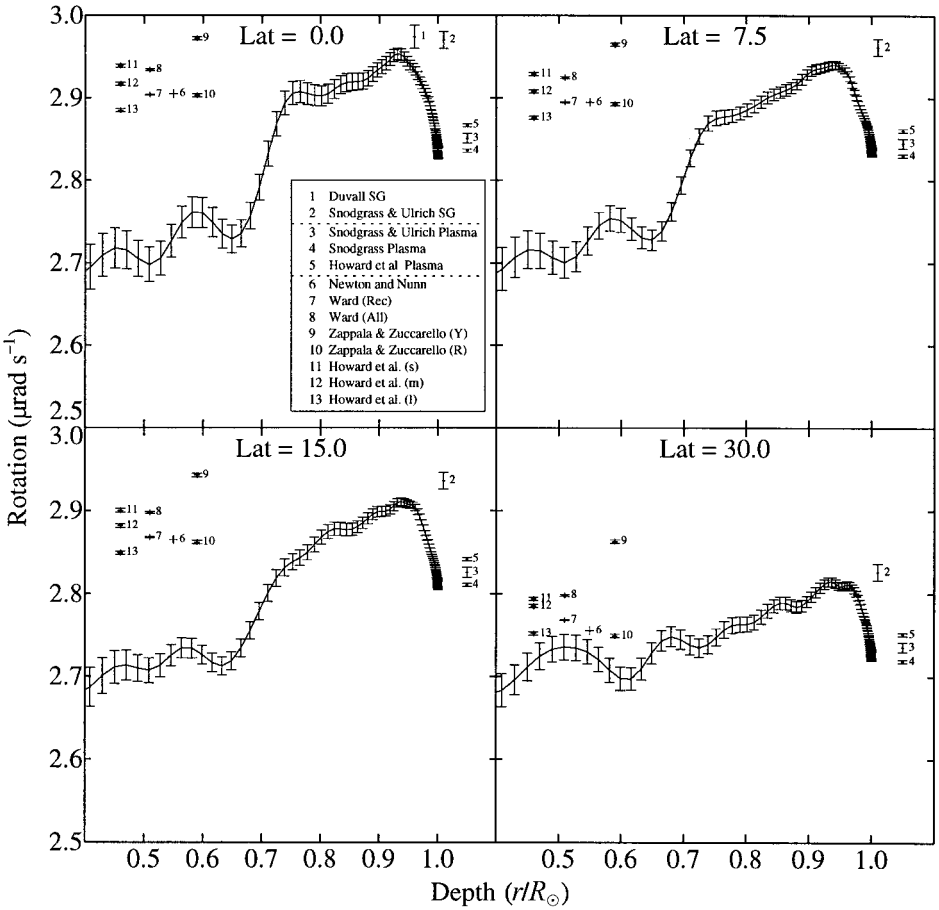

Figure 8. Comparison of rotation inversions with surface rotations. This figure compares surface measurements of solar rotation with the results of the MDI inversions for four latitudes. The ordinate axis shows the depth of the inversion; the surface measurements are grouped in the horizontal direction according to measurement type. The sunspot rotation rates are grouped to the left of each plot; the supergranulation and photospheric plasma rates measurements are grouped to the right. Most notably, both supergranulation rotation rates and the young sunspots rates observed by Z&Z are greater than the maximum rotation of the inversion. Allowing for some smoothing due to the depth and latitudinal extent of the averaging kernels, the supergranule rotation corresponds most closely to 0.93 $R_\odot$ (or a depth of 50 Mm). Recurrent sunspots rotate at rates corresponding to the rotation rates of plasma found either deeper or shallower than the peak.

to mid latitudes makes the determination of depth quite precise. It is difficult to envision supergranules as convection cells arising from 0.98 $R_\odot$ to the surface and yet rotating 3% faster than the surrounding material.

Alternate explanations of supergranulation include inertial waves (or inertial waves coupled with convection) such as Wolff (1995) and Wolff (1996). Wolff predicts Rossby-like oscillations, termed *r* modes, that modulate convective motions

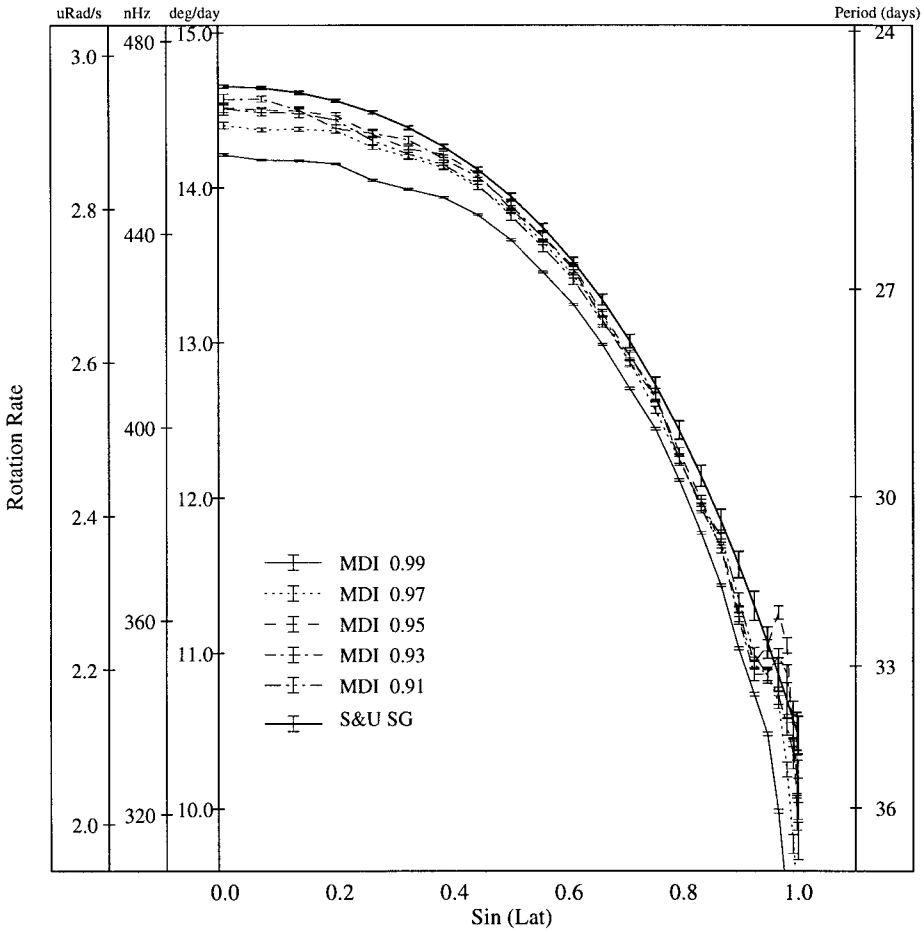

Figure 9. Rotation inversions and supergranule rotations. The results of rotation inversions for depths of 7, 21, 35, 49, and 63 Mm are shown along with the Snodgrass and Ulrich (1990) supergranulation rotation measurement. At low latitudes, the rotation rates increase with depth to 0.93 $R_\odot$ and the supergranulation rotation is significantly faster than the rotation at this depth. At mid to high latitudes supergranulation rotation remains faster than the rotation at all depths, but the statistical significance of this difference (as determined by the width of the error bars) is less.

at a depth of 0.932 $R_\odot$, which would produce cells of the approximate size and lifetime of supergranules. An interesting additional feature of *r* modes is that the propagation speed is a function of spherical harmonic degree, so the waves can appear to be rotating either faster or slower than the medium of a rotating sphere. If *r* modes do, in fact, modulate convection, the modification to the rotation speed could account for some of the discrepancy between the supergranule rotation rate and the peak inversion rate.

However, the theory of inertial waves in a differentially-rotating sphere remains imperfect, so predictions must be weighed carefully. It is, therefore, wise to in-

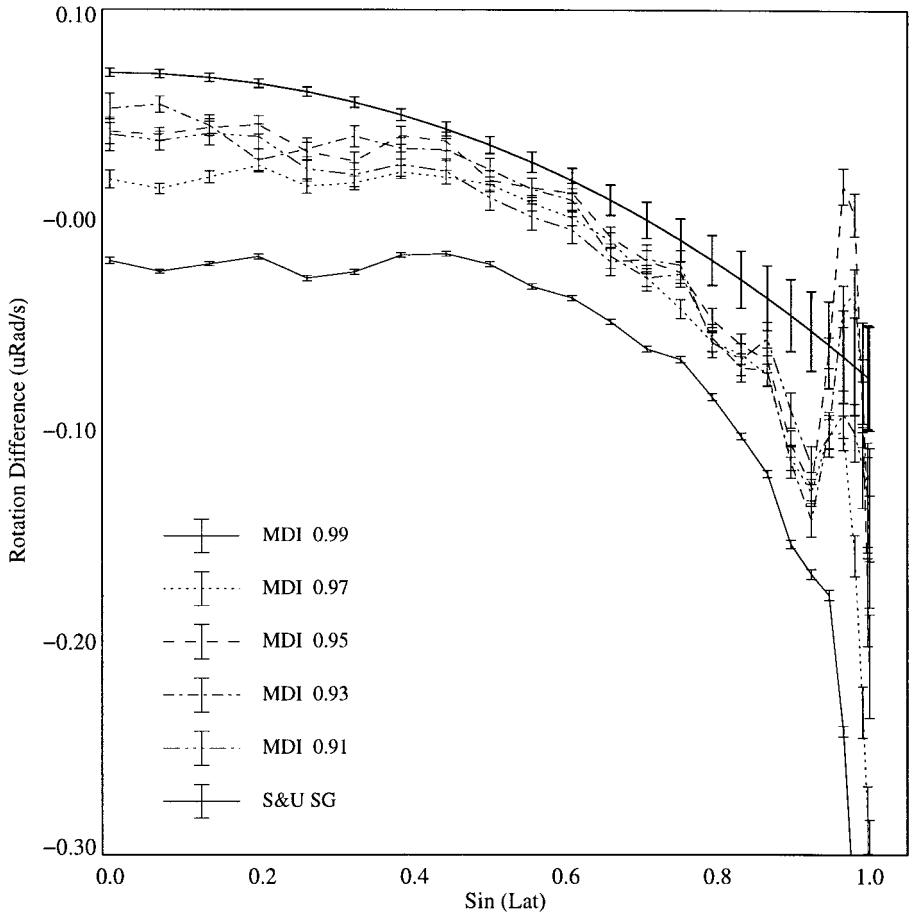

Figure 10. Differences of rotation inversions with supergranule rotations. A 'standard' differential rotation curve ($2.90 - 0.35(\sin^2\phi + \sin^4\phi)$) has been subtracted from curves plotted in Figure 9 to better show the differences. The supergranulation rotation rate is clearly significantly higher than the rotation rates within the convection zone at low latitudes. At higher latitudes there is very little overlap of error bars.

vestigate alternate explanations for the super-rotating nature of supergranules. It is clear that the simple convective model of supergranules does not explain the rotation rate.

6. Conclusion

Recent measurements of the rotation of the plasma at the solar surface are converging to a well determined rate which is slower than the rotation within the convection zone. Further, magnetic and Doppler tracers rotate faster than does the solar surface.

The comparison of tracer rotation rates with rates obtained from helioseismology may suggest anchor depths of the tracers. This interpretation yields an anchor depth of 0.93 $R_\odot$ for young sunspots and more shallow depths for older spots. A possible explanation of this may be that sunspots 'disconnect' from the subsurface magnetic field and then drift at rates comparable to the surface rates (Scherrer, 1998). However, this interpretation would indicate that sunspots are much shallower than previously expected. Alternatively, the differences in sunspot rotation rates may be due to flux tube dynamics, with the mean rate for all sizes and ages of sunspots depending on the sunspot anchor depth.

The comparison of supergranulation rotation with subsurface rotation cannot be reconciled as an anchor depth: supergranules rotate more quickly than any depth within the convection zone. The depth of 0.93 $R_\odot$ rotates the closest to the supergranule rate, but it is too deep for conventional wisdom regarding supergranules as convection cells: the simple view of supergranules does not work. Perhaps, inertial waves may explain the heightened supergranule rotation rate. Currently there is no good model which accounts for this. Perhaps, the explanation lies with more complicated theories of convection in which cells can originate from greater depths or can rotate at a rate beyond the rate of the surrounding plasma.

Acknowledgements

The author is grateful to T. L. Duvall, Jr. for his advice and many constructive comments regarding the manuscript. This research is supported by the SOI-MDI NASA grant NAS5-3077 at Stanford University.

References

Antonucci, E., Hoeksema, J. T., and Scherrer, P. H.: 1990, *Astrophys. J.* **360**, 296.
Balthasar, H., Schüssler, M. and Wöhl, H.: 1982, *Solar Phys.* **76**, 21.
Beck, J. G., Duvall, T. L., Jr., and Scherrer, P. H.: 1998, *Nature* **394**, 653.
Birch, A. C. and Kosovichev, A. G.: 1998, *Astrophys. J.* **503**, L187.
Bumba, V. and Klvaňa, M.: 1994, *Solar Phys.* **153**, 437.
Canuto, V. M., Minotti, F. O., and Schilling, O.: 1994, *Astrophys. J.* **425**, 303.
Carrington, R. C.: 1863, '*Observations of the Spots on the Sun from November 9, 1853 to March 24, 1861 Made at Redhill*', Williams and Norgate, London.
Deubner, F.-L., Ulrich, R. K., and Rhodes, E. J., Jr.: 1979, *Astron. Astrophys.* **72**, 177.
D'Silva, S. and Howard, R.: 1994, *Solar Phys.* **151**, 213.
Duvall, T. L., Jr.: 1980, *Solar Phys.* **66**, 213.
Duvall, T. L., Jr.: 1982, *Solar Phys.* **76**, 137.
Duvall, T. L., Jr.: 1998, in S. Korzennik and A. Wilson (eds.), *Structure and Dynamics of the Interior of the Sun and Sun-like Stars*, **SP-418**, 581.
Duvall, T. L., Jr. and Svalgaard, L.: 1978, *Solar Phys.* **56**, 463.
Erofeev, D. V.: 1996, *Solar Phys.* **167**, 25.
Gilman, P. A.: 1977, *Astron. Astrophys.* **58**, 315.

Gilman, P. A. and Howard, R.: 1984, *Astrophys. J.* **283**, 385.
Gilman, P. A. and Howard, R.: 1985, *Astrophys. J.* **295**, 233.
Hart, A. B.: 1954, *Monthly Notices Royal Astron. Soc.* **114**, 17.
Harvey, J. W., Hill, F., Hubbard, R. P., Kennedy, J. R., Leibacher, J. W., Pintar, J. A., Gilman, P. A., Noyes, R. W., Title, A. M., Toomre, J., Ulrich, R. K., Bhatnagar, A., Kennewell, J. A., Marquette, W., Patrón, J., Saá, O., and Yasukawa, E.: 1996, *Science* **272**, 1284.
Howard, R.: 1984, *Ann. Rev. Astron. Astrophys.* **22**, 131.
Howard, R. and Harvey, J.: 1970, *Solar Phys.* **12**, 23.
Howard, R. and LaBonte, B. J.: 1980, *Astrophys. J.* **239**, 33L.
Howard, R., Boyden, J. E., and LaBonte, B. J.: 1980, *Solar Phys.* **66**, 167.
Howard, R., Gilman, P. A., and Gilman, P. I.: 1984, *Astrophys. J.* **283**, 373.
Howard, R., Tanenbaum, A. S., and Wilcox, J. M.: 1968, *Solar Phys.* **4**, 286.
Howard, R., Adkins, J. M., Boyden, J. E., Gragg, T. A., Gregory, T. S., LaBonte, B. J., Padilla, S. P. and Webster, L.: 1983, *Solar Phys.* **83**, 321.
Kambry, M. A. and Nishikawa, J.: 1990, *Solar Phys.* **126**, 89.
Komm, R. W., Howard, R. F., and Harvey, J. W.: 1993a, *Solar Phys.* **143**, 19.
Komm, R. W., Howard, R. F., and Harvey, J. W.: 1993b, *Solar Phys.* **145**, 1.
LaBonte, B. J. and Howard, R.: 1982, *Solar Phys.* **80**, 361.
Meunier, N.: 1999, *Astrophys. J.* **515**, 801.
Nesme-Ribes, E., Ferreira, E. N., and Mein, P.: 1993 *Astron. Astrophys.* **274**, 563.
Newton, H. W. and Nunn, M. L.: 1951, *Monthly Notices Roy. Astron. Soc.* **111**, 413.
Rhodes, E. J., Cacciani, A., Korzennik, S., Tomczyk, S., Ulrich, R. K., and Woodard, M. F.: 1990, *Astrophys. J.* **351**, 687.
Riehokainen, A., Urpo, S., and Valtaoja, E.: 1998, *Astron. Astrophys.* **333**, 741.
Rüdiger, G.: 1989, *Differential Rotation and Stellar Convection* (Akademie-Verlag, Berlin, GDR).
Scherrer, P. H.: 1998, private communication.
Scherrer, P. H., Wilcox, J. M., and Svalgaard, L.: 1980, *Astrophys. J.* **241**, 811.
Scherrer, P. H., Bogart, R. S., Bush, R. I., Hoeksema, J. T., Kosovichev, A. G., Schou, J., Rosenberg, W., Springer, L., Tarbell, T. D., Title, A., Wolfson, C. J., Zayer, I. and the MDI engineering team: 1995, *Solar Phys.* **162**, 129.
Scherrer, P. H., Schou, J., Bogart, R. S., Bush, R. I., Hoeksema, J. T., Kosovichev, A. G., Antia, H. M., Chitre, S. M., Christensen-Dalsgaard, J., Larsen, R. M., Pijpers, F. P., Eff-Darwich, A., Korzennik, S. G., Gough, D. O., Sekii, T., Howe, R., Tarbell, T. D.,Title, A. M., Thompson, M. J., and Toomre, J.: 1997, *Bull. Am. Astron. Soc.* **191**, No. 73.10.1
Schmidt, W.: 1982, *Geophys. Astrophys. Fluid Dyn.* **21**, 27.
Schou, J., Christensen-Dalsgaard, J., and Thompson, M. J.: 1994, *Astrophys. J.* **433**, 389.
Schou, J., Antia, H. M., Basu, S., Bogart, R. S., Bush, R. I., Chitre, S. M., Christensen-Dalsgaard, J., Di Mauro, M. P., Dziembowksi, W. A., Eff-Darwich, A., Gough, D. O., Haber, D. A., Hoeksema, J. T., Howe, R., Korzennik, S. G., Kosovichev, A. G., Larsen, R. M., Pijpers, F. P., Scherrer, P. H., Sekii, T., Tarbell, T. D., Title, A. M., Thompson, M. J., and Toomre, J.: 1998, *Astrophys. J.* **505**, 390.
Schröter, E. H.: 1985, *Solar Phys.* **100**, 141.
Simon, G. W. and Weiss, N. O.: 1968, *Z. Astrophys.* **69**, 435.
Snodgrass, H. B.: 1983, *Astrophys. J.* **270**, 288.
Snodgrass, H. B.: 1984, *Solar Phys.* **94**, 13.
Snodgrass, H. B. and Ulrich, R. K.: 1990, *Astrophys. J.* **351**, 309.
Snodgrass, H. B., Howard, R., and Webster, L.: 1984, *Solar Phys.* **90**, 199.
Stix, M.: 1989, in G. Klare (ed.), *Reviews in Modern Astronomy*, Springer-Verlag, Berlin. p. 248.
Tang, F.: 1981, *Solar Phys.* **69**, 399.
Thompson, M. J., Toomre, J., Anderson, E. R., Antia, H. M., Berthomieu, G., Burtonclay, D., Chitre, S. M., Christensen-Dalsgaard, J., Corbard, T., DeRosa, M., Genovese, C. R., Gough, D. O.,

Haber, D. A., Harvey, J. W., Hill, F., Howe, R., Korzennik, S. G., Kosovichev, A. G., Leibacher, J. W., Pijpers, F. P., Provost, J., Rhodes, E. J., Jr., Schou, J., Sekii, T., Stark, P. B., and Wilson, P. R.: 1996, *Science* **272**, 1300.
Ulrich, R. K.: 1970, *Astrophys. J.* **162**, 933.
Ulrich, R. K.: 1998, in S. Korzennik and A. Wilson (eds.), *Structure and Dynamics of the Interior of the Sun and Sun-like Stars*, **SP-418**, 851.
Ulrich, R. K. and Bertello, L.: 1996, *Astrophys. J.* **465**, L65.
Ulrich, R. K., Boyden, J. E., Webster, L., Snodgrass, H. B., Padilla, S. P., Gilman, P., and Shieber, T.: 1988, *Solar Phys.* **117**, 291.
Ward, F.: 1966, *Astrophys. J.* **145**, 416.
Wilcox, J. M., Schatten, K. H., Tanenbaum, A. S., and Howard, R.: 1970, *Solar Phys.* **14**, 255.
Wolff, C. L.: 1995, *Astrophys. J.* **443**, 423.
Wolff, C. L.: 1996, *Astrophys. J.* **459**, L103.
Zahn, J.-P., Talon, S., and Matias, J.: 1997, *Astron. Astrophys.* **322**, 320.
Zappala, R. A. and Zuccarello, F.: 1991, *Astron. Astrophys.* **242**, 480.